Yang et al. *Zool. Res.* 2022, 43(6): 911−922
https://doi.org/10.24272/j.issn.2095-8137.2022.220

ZR | Zoological Research

Article Open Access

OCT6 inhibits differentiation of porcine-induced pluripotent stem cells through MAPK and PI3K signaling regulation

Xin-Chun Yang[1,#], Xiao-Long Wu[1,#], Wen-Hao Li[1], Xiao-Jie Wu[1], Qiao-Yan Shen[1], Yun-Xiang Li[1], Sha Peng[1], Jin-Lian Hua[1,*]

[1] *College of Veterinary Medicine*, *Shaanxi Centre of Stem Cells Engineering* & *Technology*, *Northwest A* & *F University*, *Yangling*, *Shaanxi* 712100, *China*

ABSTRACT

As a transcription factor of the Pit-Oct-Unc (POU) domain family, octamer-binding transcription factor 6 (*OCT6*) participates in various aspects of stem cell development and differentiation. At present, however, its role in porcine-induced pluripotent stem cells (piPSCs) remains unclear. Here, we explored the function of *OCT6* in piPSCs. We found that piPSCs overexpressing *OCT6* maintained colony morphology and pluripotency under differentiation conditions, with a similar gene expression pattern to that of non-differentiated piPSCs. Functional analysis revealed that *OCT6* attenuated the adverse effects of extracellular signal-regulated kinase (ERK) signaling pathway inhibition on piPSC pluripotency by activating phosphatidylinositol 3-kinase-protein kinase B (PI3K-AKT) signaling activity. Our research sheds new light on the mechanism by which *OCT6* promotes PSC maintenance.

Keywords: *OCT6*; piPSCs; MAPK/ERK; PI3K/AKT; Pluripotency

INTRODUCTION

Octamer-binding factor 6 (Oct-6, Pou3f1, SCIP, Tst-1) is a transcription factor of the Pit-Oct-Unc (POU) family (Wu et al., 2010). The DNA-binding (POU) domain of these proteins is highly conserved, consisting of a POU-specific domain and a POU homeodomain (Sock et al., 1996). POU transcription factors recognize the common DNA octamer motif (ATGCAAAT) (Jauch et al., 2011). They play distinct roles in stem cell development and function and exhibit spatiotemporal expression patterns (Kim et al., 2020). *OCT6* is not widely expressed in all cells but has been detected in embryonic stem cells (ESCs) (Meijer et al., 1990), Schwann cells (Friedrich et al., 2005), glial cells (Kuhlbrodt et al., 1998), and neonatal testicular cells (Wu et al., 2010). To date, most studies have explored the function of *OCT6* in Schwann cells, while little is known regarding their functions in other cell types. For induced pluripotent stem cells (iPSCs), *OCT6* partially replaces *OCT4* to initiate reprogramming (Jerabek et al., 2017). *OCT6* is also implicated in the maintenance of iPSC pluripotency and plays a decisive role in neural differentiation (Malik et al., 2019). However, few studies have investigated the potential functions and mechanisms of *OCT6* in porcine iPSCs (piPSCs).

The mitogen-activated protein kinase (MAPK) signaling pathway regulates many biological processes, including cell cycle, apoptosis, differentiation, protein biosynthesis, and

Received: 01 July 2022; Accepted: 01 September 2022; Online: 02 September 2022

Foundation items: This work was supported by the National Natural Science Foundation of China (32072806), Shaanxi Province Science and Technology Innovation Team Project (2019TD-036), and Shaanxi Province Science and Technology Project (2022NY-044)

#Authors contributed equally to this work

*Corresponding author, E-mail: jinlianhua@nwsuaf.edu.cn

tumorigenesis (Wen et al., 2022). Activation of the mitogen-activated protein/extracellular signal-regulated kinase (MEK) signaling pathway can promote differentiation of mouse ESCs (mESCs), while inhibition of MEK/ERK signal transduction can promote self-renewal and pluripotency of mESCs (Choi et al., 2017). Inhibition of MEK facilitates transformation of mouse ectodermal stem cells into ESC-like cells, however inhibition of the MEK signaling pathway reduces pluripotency in porcines (Xu et al., 2019). Previous reports have indicated that piPSCs differ from mESCs. Inhibition of MAPK impairs piPSC pluripotency and decreases cell proliferation ability (Zhu et al., 2021). Phosphatidylinositol 3-kinase (PI3K), a dimer consisting of a regulatory subunit p85 and catalytic subunit p110 (Aoki & Fujishita, 2017), activates protein kinase B (AKT), thereby regulating cell proliferation, differentiation, apoptosis, and migration (Haddadi et al., 2018). PI3K/AKT plays a vital role in maintaining ESC self-renewal (Yao et al., 2010). Interestingly, impairment of pluripotency by inhibiting MEK in mouse ESCs can be counteracted by PI3K activation (Singh et al., 2012).

We previously reported that porcine PSCs can be induced in medium containing leukemia inhibitory factor (LIF), basic fibroblast growth factor (bFGF), and other cytokines, with the addition of signal transduction inhibitors (Chir099021, SB431542) and feeder cells to maintain colony morphology and pluripotency (Ma et al., 2018). Here, as *OCT6* is not expressed in piPSCs, we explored the function of *OCT6* in piPSCs by its overexpression. Notably, piPSCs overexpressing *OCT6* showed smoother colony edges in the presence of feeder cells (feeders) and maintained normal colony morphology and pluripotency after feeder removal. RNA sequencing (RNA-seq) analysis revealed that *OCT6* expression promoted the up-regulation of extracellular matrix (ECM)-related genes and inhibited the differentiation of piPSCs. In addition, *OCT6* activated PI3K and inhibited ERK in piPSCs, consistent with its ability to maintain piPSC colony morphology and pluripotency upon feeder removal.

MATERIALS AND METHODS

Overall experimental scheme

In this study, we used lentivirus packaging to transfect PCDH-Teton-3×Flag-*OCT6*-Puro and PCDH-Teton-3×Flag-Puro into piPSCs. The piPSCs transfected with the *OCT6* gene vector (OE-OCT6 piPSCs) were used as the experimental group, and the piPSCs transfected with empty vector (OE-NC piPSCs) were used as the control group. *OCT6* expression was detected by quantitative real-time polymerase chain reaction (qRT-PCR), cellular immunofluorescence staining, and western blot analysis. We performed total RNA-seq of piPSCs and detected the expression levels of related genes using qRT-PCR, western blotting, and immunofluorescence staining. Small molecular compounds were used to activate or inhibit the ERK and PI3K-AKT signaling pathways, respectively, to compensate for the maintenance of pluripotency caused by overexpression of *OCT6*.

Acquisition and production of piPSCs

The piPSCs were obtained from previous research. We established doxycycline (Dox)-induced porcine PSCs, in which the expression of transgenic genes can be switched on/off by Dox and lentiviral particles of TetO-FUW-OSKM (*OCT4*, *SOX2*, *KLF4*, and *c-MYC*) and FUW-M2rtTA can be infected into porcine embryonic fibroblasts (PEFs). Here, the somatic cells were reprogrammed into porcine iPSCs induced by Dox (DOX-iPSCs), which displayed a normal karyotype of 38 chromosomes, formed embryonic bodies *in vitro*, and spontaneously differentiated into three germ layers (Ma et al., 2018).

Cell culture

HEK293T cells were cultured in 6-well plates (Thermo Fisher Scientific, USA) using Dulbecco's Modified Eagle Medium (DMEM) (Corning, USA) and 10% fetal bovine serum (FBS) (Gibco, USA) at 37 ℃ with 5% CO_2, with new medium changed each day. Mouse embryonic fibroblasts (MEFs) were cultured with DMEM supplemented with 10% FBS, then treated with mitomycin C for 3 h and cultured on a 12-well plate (1×10^5 cells/well) at 37 ℃ with 5% CO_2. The piPSCs were cultured in DMEM (Corning, USA) supplemented with 15% FBS (Vistech, New Zealand), 10 ng/mL LIF (Sino Biological, China), 10 ng/mL bFGF (10014-HNAE, Sino Biological, China), 0.1 mmol/L L-glutamine, 3 μmol/Lol/L CHIR99021 (M3148, Sigma-Aldrich, USA), 2 μmol/Lol/L SB431542 (S1067, Selleck, USA), 0.1 mmol/L β-mercaptoethanol (M3148, Sigma-Aldrich, USA), 4 μg/mL doxycycline (D9891, Sigma-Aldrich, USA), 100 μg/mL streptomycin, 100 U/mL penicillin, and 0.1 mmol/L non-essential amino acids (NEAA) (Gibco, USA) at 37 ℃ with 5% CO_2. After the piPSCs were grown to 80%–90% confluency, they were digested into single cells on a 12-well plate (2×10^4 cells/well) using TrypLE Select (Gibco, USA) (Wu et al., 2021; Zhu et al., 2021).

Vector construction and cloning

To explore the function of *OCT6* in piPSCs, total RNA was extracted from porcine testes using TRIzol Reagent (Takara, Japan), then reverse transcribed (Thermo Fisher Scientific, USA) into cDNA. The porcine *OCT6* gene was PCR-amplified from cDNA, and subcloned into an in-house PCDH-Teton-3×Flag-MCS-Puro vector using a NovoRec® plus One step PCR Cloning Kit (Novoprotein, China). All primers used in this study are provided in Supplementary Table S1, and the core coding sequence of the recombinant vector was verified by sequencing.

Lentiviral packaging

After HEK293T cells were grown to 80%–90% density in 6-well plates, lentiviral plasmids (VSV-G, PAX2) for packaging were transfected into the cells using polyethyleneimine (PEI). In total, 1 μg of VSV-G, 1 μg of PAX2, and 2 μg of lentiviral plasmids were mixed with 12 μL of PEI (1 mg/mL), rested for 15 min, followed by the addition of 200 μL of Opti-MEM to the HEK293T cells. After 12 h, the culture medium was changed to DMEM. After 48–72 h, the lentiviral particles were collected, and cell fragments were filtered with a 0.45 μmol/L filter. Viruses were used after 12 h of rest at 4 ℃.

Lentiviral particle transduction

The passaged piPSCs were inoculated into a 12-well plate

covered with feeders. The viral supernatant containing lentiviral particles was mixed with the piPSC culture medium (1:1) and 4 μg/mL polystyrene. The piPSCs in mixed medium were cultured at 37 ℃ for 8–12 h, after which the medium was replaced with new piPSC medium. Puromycin was used to select purine-positive cells after 7 days of culture.

RNA extraction, reverse transcription, and qRT-PCR detection

RNAiso Plus Reagent (Takara, Japan) was selected to extract total RNA. Quality of the extracted RNA was detected using a Nanodrop microspectrophotometer (Thermo Fisher Scientific, USA) and agarose gel electrophoresis. After removing the feeders, the cells were passaged once to remove feeder interference, followed by total RNA extraction. The RNA (2 μg) was then reverse transcribed using a RevertAid First-Strand cDNA Synthesis Kit (Thermo Fisher Scientific, USA) to obtain cDNA. Finally, qRT-PCR was performed through a three-step process using SuperReal PreMix Plus (SYBR Green) (Tiangen, China) (Wei et al., 2021). The primers for qRT-PCR are shown in Supplementary Table S1.

Immunofluorescence staining

The piPSCs were washed twice with phosphate-buffered saline (PBS) and fixed at room temperature for 15 min with 4% paraformaldehyde. The cell membrane was perforated with 0.1% Triton-100 for 10 min, then sealed at room temperature for 1 h with 10% FBS. The cells were incubated with primary antibodies (Flag; 1:1 000; Sigma-Aldrich, USA) at 4 ℃ for 12 h, then washed with PBS three times and incubated with goat anti-mouse IgG (H+L) secondary antibody AlexaFluor488 (1:500; ZSGB-BIO, China) conjugated at room temperature for 1 h. Cells were counterstained at room temperature with Hoechst33342 (1:1 000) for 5 min. Finally, images were collected using an EVOS fluorescence microscope (Thermo Fisher Scientific, USA).

Western blot analysis

The piPSCs (~80% density) were digested using TrypLE™ Select (Thermo Fisher Scientific, USA), with the same volume of DMEM and 10% FBS then added to neutralize the digestion reaction. The cell mixture was transferred into a 1.5 mL EP tube and centrifuged at 5 000 ×*g* for 3 min at 24 °C to obtain the cell precipitation. RIPA lysate (Beyotime, China), 10 mmol/L PMSF protease inhibitor (Sigma-Aldrich, USA), and phosphatase inhibitor were used to cleave the piPSCs on ice for 30 min. After that, 5×sodium dodecyl-sulfate polyacrylamide gel electrophoresis (SDS-PAGE) loading buffer was added for denaturation at 100 °C for 5 min. The protein sample was transferred to 8%–12% SDS-PAGE gel for separation at 100 V. The gel was then transferred to a Trans-Blot SD Cell and System (Bio-Rad, USA) and to polyvinylidene fluoride (PVDF) membranes at a voltage of 15 V. The membranes were sealed at room temperature with 8% skim milk or 5% bovine serum albumin (BSA) for 2 h, then incubated at 4 ℃ for 12 h with primary antibodies, including β-actin (1:8 000; AbMole, USA), Flag (1:1 000; Sigma-Aldrich, USA), OCT6 (1:1 000; Abmart, China), phospho-p44/42 MAPK (1:1 000; Cell Signaling Technology, USA), p44/42 MAPK (1:1 000; Cell Signaling Technology, USA), PI3K-AKT (1:2 000; Abmart, China), and phospho-PI3K-AKT (1:2 000; Abmart, China). All primary antibodies were diluted with TBST buffer (20 mmol/L Tris HCl/pH 8.0, 150 mmol/L NaCl, 0.05% Tween 20).

The PVDF membranes were washed in TBST buffer for 30 min, and new TBST buffer was replaced every 10 min. The membranes were incubated with goat anti-mouse/rabbit IgG (H+L) (Cell Signaling Technology, USA) at 37 ℃ for 1 h, then washed with TBS-T buffer at room temperature for 15 min. Finally, the Tanon-5200 automatic chemiluminescence image analysis system (Tanon, China) was used to detect horseradish peroxidase (HRP) signals. ImageJ (v1.53c) was used to analyze the relative grayscale of western blots.

Alkaline phosphatase (AP) staining

Suitable piPSCs were fixed with 4% paraformaldehyde (pH 7.4) for 15 min, then washed 2–3 times with PBS. The cells were stained with AST Fast Red TR and α-naphthol AS MX phosphate (Sigma-Aldrich, USA) according to the manufacturer's instructions. In brief, 1.0 mg/mL AST Fast Red TR, 0.4 mg/mL α-naphthol AS MX phosphate, and 0.1 mmol/L Tris-HCL 8.8 buffers were used to prepare the AP staining solution. The cells were incubated for 20 min with AP stain, which was then replaced with PBS. The AP-positive piPSC clones showed red and images were captured using a phase contrast microscope (Nikon, Japan).

RNA-seq analysis

To explore the molecular mechanism of *OCT6* in piPSCs, we performed RNA-seq of OE-OCT6 and OE-NC piPSCs after feeder removal (Zhu et al., 2021). We extracted total RNA using RNAisoPlus Reagent (Takara, Japan) and guanidine isothiocyanate phenol-chloroform extraction. Total RNA quality was detected using a Nanodrop spectrophotometer, and total RNA integrity was detected by agarose gel electrophoresis. Total RNA was digested using DNase Ⅰ, mRNA was enriched using Oligo (dT) magnetic beads, and cDNA was synthesized by adding random primers after mRNA was interrupted (second-strand cDNA was synthesized with dUTP instead of dTTP). Next, 3'adenylated and adaptor ligation was performed at the ends of the synthesized double-stranded DNA. Joint connection and PCR amplification of the connection products were carried out. A DNA library was constructed and quality-checked, with the resulting product then cyclized (Yu et al., 2021). The DNBSEQ platform was used for computer sequencing, and quality control (QC) of the obtained raw reads was carried out. The filtered clean reads were compared to the porcine genome Ssc11.1, and expression level was normalized to reads per kilobase per million mapped reads (RPKM) using gene annotation files. EdgeR was used to analyze differences in samples. Heat-maps were drawn using pheatmap (v1.0.12) to show specific gene expression levels. ClusterProfiler (v4.2.2) was used for Gene Ontology (GO) and Kyoto Encyclopedia of Genes and Genomes (KEGG) analysis. Adjusted $P<0.05$ or $Q<0.05$ was used to define the working threshold of statistical significance.

Statistical analysis

Student *t*-test was used to determine significant differences between two groups, and univariate or multivariate analysis of

variance (ANOVA) was used to determine significant differences between multiple groups. All data were expressed as mean±standard error (*SE*) and differences were considered significant at $P<0.05$.

RESULTS

Cloning and overexpression of porcine *OCT6* gene in piPSCs

To determine whether overexpression of *OCT6* can improve the anti-differentiation ability of piPSCs, we introduced the *OCT6* gene cloned from porcine testicular tissue into the lentiviral vector. The *OCT6* protein sequence was highly conserved, with only three amino acid differences among *Homo sapiens*, *Mus musculus*, and *Sus scrofa* (Figure 1A).

To further investigate the role of porcine *OCT6* in piPSCs, we generated piPSC lines stably expressing porcine *OCT6* using the TetOn lentiviral vector (Figure 1B). Quantitative analysis showed that the *OCT6* gene was up-regulated (1.25×10^4 times) compared with the negative control (NC, TetOn-3×Flag empty vector). After three consecutive passages, AP staining was performed. Results showed that overexpression of *OCT6* did not affect piPSC pluripotency, and the edge of the piPSC clones was smoother than that of the NC (Figure 1D). Both protein and immunofluorescence analyses showed that the OCT6 protein expression was significantly up-regulated in *OCT6* piPSCs but could not be detected by Flag or OCT6 antibodies in the NC group (Figures 1E, F). These results suggest that *OCT6* helps maintain colony morphology of piPSCs.

OCT6 inhibits piPSC differentiation under differentiation conditions

We then applied differentiation conditions to verify the role of *OCT6* in maintaining piPSC morphology and pluripotency (Kim et al., 2020, 2021; Wu & Yao, 2005). Under differentiation conditions, the piPSCs overexpressing *OCT6* maintained basic colony morphology for three consecutive passages without feeders (Figure 2A). AP staining was used to determine the effects of *OCT6* on piPSC pluripotency under differentiation conditions. Results showed that piPSCs overexpressing *OCT6* maintained pluripotency, even in the culture system without feeders (Figure 2B). Detection of core pluripotent genes showed a slight but significant increase in exogenous OSKM and endogenous *OCT4* expression (1.31 and 1.86 times, respectively) and an obvious up-regulation in endogenous *c-Myc* expression (2.92 times) in the OE-OCT6 piPSCs (Figure 2C). Previous studies have shown that *c-Myc* is the downstream target of the Wingless/Integrated (WNT) signaling pathway, and an increase in *c-Myc* gene expression may be related to activation of WNT (Yu et al., 2019; Zhang et al., 2021). We therefore removed the GSK3 inhibitor Chir99021 from the culture medium. However, results showed that OE-OCT6 still maintained colony morphology and pluripotency after Chir99021 removal (Figure 2D).

To further explore the results caused by overexpression of *OCT6*, we performed RNA-seq of the two piPSC lines after 5 days of culture. Results showed that transcriptional changes occurred in both directions after overexpression of *OCT6* (339 up-regulated genes and 639 down-regulated genes) (Figure 2E). We detected pluripotency-related genes by qRT-PCR and found that compared with the OE-NC group, the OE-OCT6 group showed elevated *c-Myc* and *OCT4* expression but inhibited *LIN28A* expression, which may be related to the inhibition of differentiation (Figure 2C). The most significant differentially expressed genes (DEGs) from RNA-seq were verified by qRT-PCR. Results showed that these hypervariable genes were involved in the inhibition of differentiation and maintenance of stem cell pluripotency. Among them, *PAX5*, *CLU*, and *COL5A1* affect differentiation (Baghdadi et al., 2018; Mansouri et al., 1996; Oh et al., 2020) and *SOX3*, *SIX6*, and *L1CAM* are involved in the regulation of stem cell pluripotency (Corsinotti et al., 2017; Son et al., 2011; Wolfrum et al., 2010) as well as decreased expression of imprinted gene *NNAT* (Teichroeb et al., 2011), with epigenetic erasure required for resetting the cell identity to a ground state, which may explain why *OCT6* overexpression is beneficial for the cloning and maintenance of pluripotency (Figure 2F).

We further carried out KEGG and GO analyses of the RNA-seq data. KEGG analysis showed that the DEGs were mainly enriched in the MAPK and PI3K-AKT signaling pathways (Figure 2G). GO analysis indicated that the DEGs were primarily related to the ECM, extracellular space, and whole composition of plasma membrane (Figure 2H). These findings suggest that *OCT6* not only affects the canonical pathways but may also inhibit piPSC differentiation by regulating the components of the ECM and cell membrane.

OCT6 maintains morphology and reduces pluripotency of piPSC colonies by inhibiting MAPK-ERK pathway

KEGG analysis was performed to explore the possible pathways regulated by *OCT6*. Results indicated that the main enriched pathways were the MAPK, PI3K-ATK, and ECM pathways. As MAPK and PI3K-AKT play important roles in piPSCs, we compared the OE-OCT6 and OE-NC groups with piPSCs cultured with (MOCK group) or without feeders (F-group). The heat-map of MAPK-related genes showed that the expression patterns in the OE-NC and F-groups and the OE-OCT6 and MOCK groups were similar (Figure 3A). The qRT-PCR results further confirmed that the gene expression pattern in the OE-OCT6 group was basically the same as that in the MOCK group, indicating that the OE-OCT6 group maintained the characteristics of piPSCs after feeder removal, and OE-OCT6 may inhibit the ERK pathway via activation of *DUSP10* and inhibition of *PTPRR*, *RRAS*, and *FGFR3* (Figure 3B, C).

Under feeder removal conditions, the ERK and phosphorylated ERK (p-ERK) protein expression levels in the OE-OCT6 piPSCs relative to the OE-NC piPSCs significantly increased and decreased, respectively (Figure 3D). We verified the changes in the MAPK-ERK pathway in piPSCs with and without feeders, which indicated that the ERK pathway was inhibited by the removal of feeders (Figure 3E). To verify this, we tested PD0325901 (ERK inhibitor) and 12-O-tetradecanoyl phorbol-13-acetate (PMA, ERK activator) in the piPSCs. When 1 μmol/L PD0325901 was added to the OE-OCT group, the colonies became smaller; in contrast, piPSCs

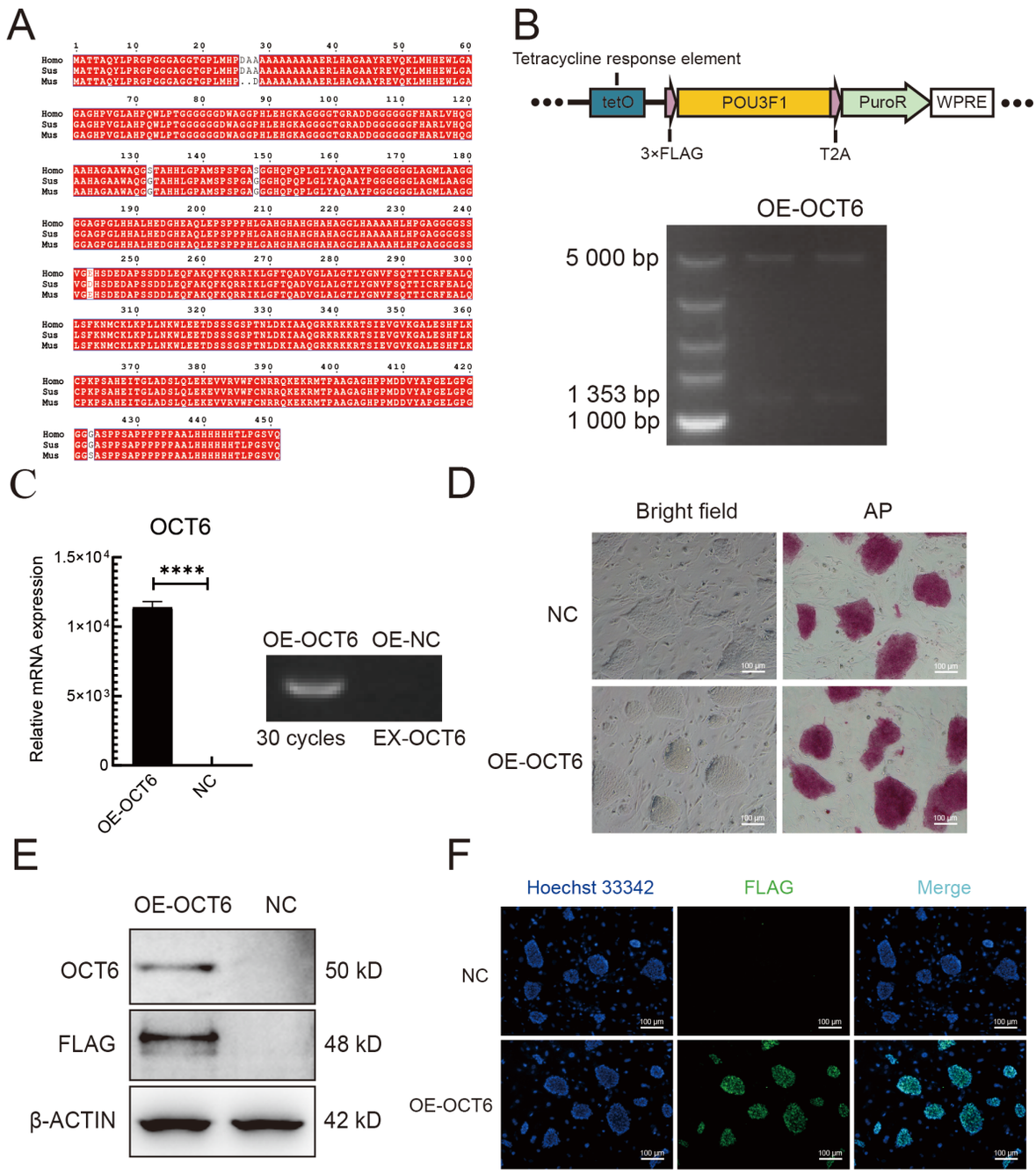

Figure 1 Cloning and overexpression of *OCT6* gene in piPSCs

A: Sequence alignment of OCT6 protein in humans, mice, and pigs. Red area indicates homogeneity of amino acid sequences among species. B: *OCT6* gene overexpression map and endonuclease digestion results. C: Left: qRT-PCR analysis of *OCT6* in OE-NC and OE-OCT6 groups. Relative expression level was normalized to β-actin. Data represent mean±*SE*; *n*=3 independent experiments. Right: Semi-quantitative RT-PCR analysis of exogenous *OCT6* (ex-*OCT6*) in OE-NC and OE-OCT6 groups. D: Representative images of OE-NC and OE-OCT6 cultured in LB2i medium with bright field and AP staining. *n*=3 independent experiments. Scale bar: 100 μm. E: Representative western blotting of OCT6 and Flag-tag was performed after 5 days of culture under specific conditions. Data represent mean±*SE*. *n*=3 independent experiments. F: NC and OE-OCT6 were analyzed by immunofluorescence-staining against Flag-tag. Nucleus was stained with DAPI. Scale bar: 100 μm. *n*=3 independent experiments.

showed obvious differentiation after the addition of PMA (Figure 3F). However, the piPSCs maintained basic colony morphology after the addition of PD0325901 (Figure 3G). These findings confirm that inhibition of ERK may be of significance for the maintenance of piPSCs. After the concentration gradient test, 1 μmol/L PD0325901 and 1

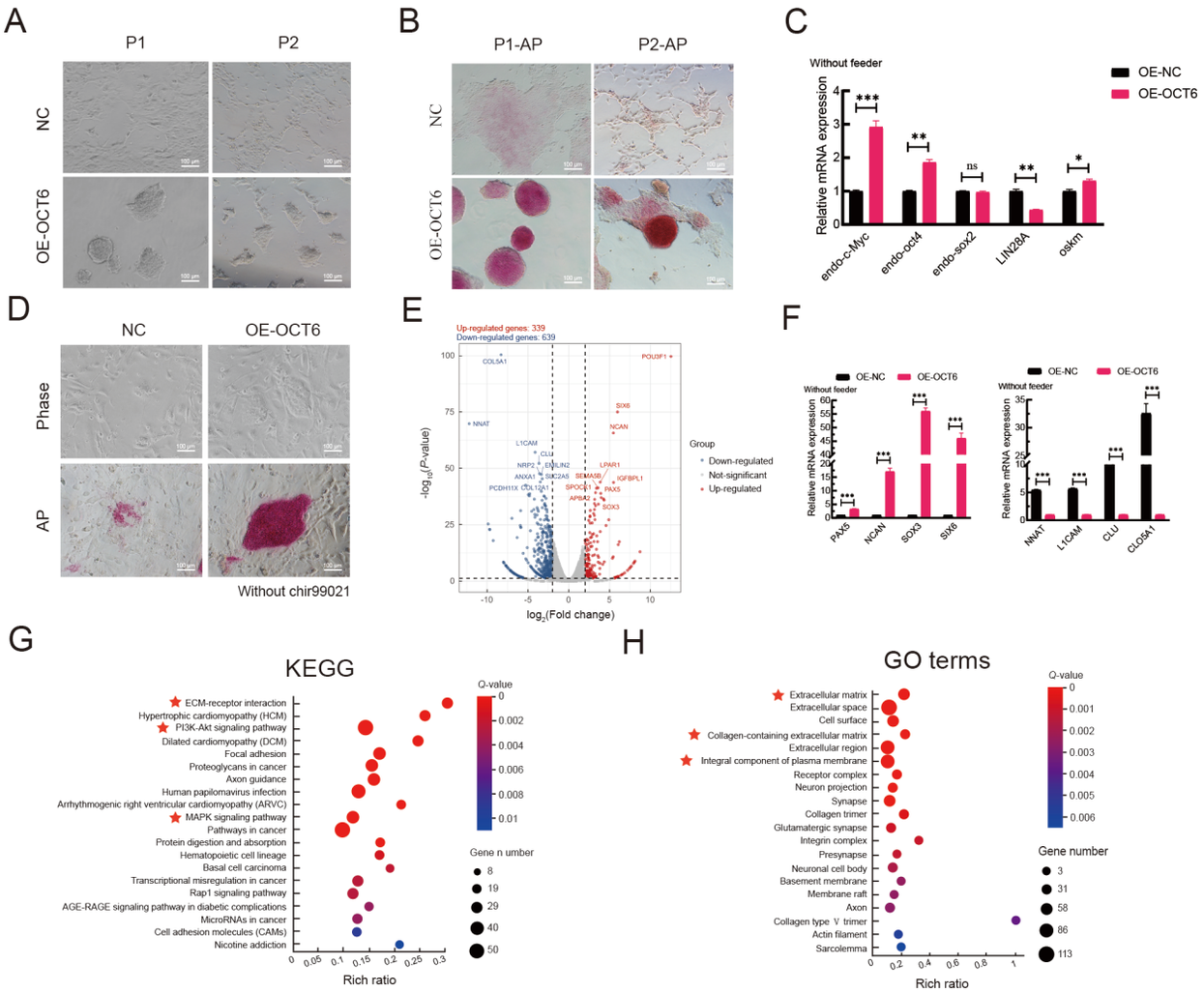

Figure 2 OE-OCT6-piPSCs maintained good colony morphology independent of feeders compared with OE-NC piPSCs

A: Representative bright field images of overexpressed control (OE-NC) and overexpressed *OCT6* (OE-OCT6) piPSC groups continuously cultured in LB2i medium for two generations after feeder removal. Scale bar: 100 μm. *n*=3 independent experiments. B: Representative AP-staining images of OE-NC and OE-OCT6 piPSC groups continuously cultured in LB2i medium for two generations after feeder removal. Scale bar: 100 μm. *n*=3 independent experiments. C: qRT-PCR analysis of endo-*c-Myc*, endo-*Oct4*, endo-*Sox2*, *LIN28A*, and ex-OSKM in OE-NC and OE-OCT6 groups. Relative expression levels were normalized by β-actin. Data represent mean±SE; *n*=3 independent experiments. D: Representative bright field and AP-staining images of OE-NC and OE-OCT6 piPSCs cultured in LB2i medium without Chir99021. *n*=3 independent experiments. Scale bar: 100 μm. E: Transcriptional profiles of piPSCs after overexpression of *OCT6*. Red represents up-regulated genes, blue represents down-regulated genes, and gray represents no significant change. F: qRT-PCR analysis of hypervariable genes, with detected genes involved in cell differentiation, neuronal differentiation, and ECM regulation. Relative expression levels were normalized to β-actin. Data represent mean±SE; *n*=3 independent experiments. G KEGG enrichment of up-regulated DEGs in OE-OCT6 group. H: GO enrichment of up-regulated DEGs in OE-OCT6 group.

μmol/L PMA were selected as the optimum concentrations for ERK inhibition and activation, respectively (Supplementary Figure S1A, B).

PI3K-AKT pathway compensates for adverse effects caused by MAPK-ERK suppression

We next asked how *OCT6* maintains piPSC pluripotency after feeder removal. Heat-map and qRT-PCR analysis showed that the expression patterns of PI3K-AKT pathway-related genes in the OE-OCT6 group were similar to those in the MOCK group (Figure 4A). Notably, expression of the *MAGI* family, *LPAR1*, and *IGTB4* genes increased, while PPP2R3A expression decreased. These genes are associated with cell adhesion and improvement in piPSC colony formation (Gong et al., 2019; Li et al., 2017b, 2019) (Figure 4B, C). In the absence of feeders, AKT and phosphorylated AKT were significantly decreased and increased, respectively, in the OE-OCT6 group relative to the OE-NC group (Figure 4D). We also compared the protein level of AKT in the OE-NC group with or without feeders and found that AKT and phosphorylated AKT were significantly decreased and increased, respectively, in the presence of feeders (Figure 4E). This change in AKT level in the OE-OCT6 group disappeared after the addition of the

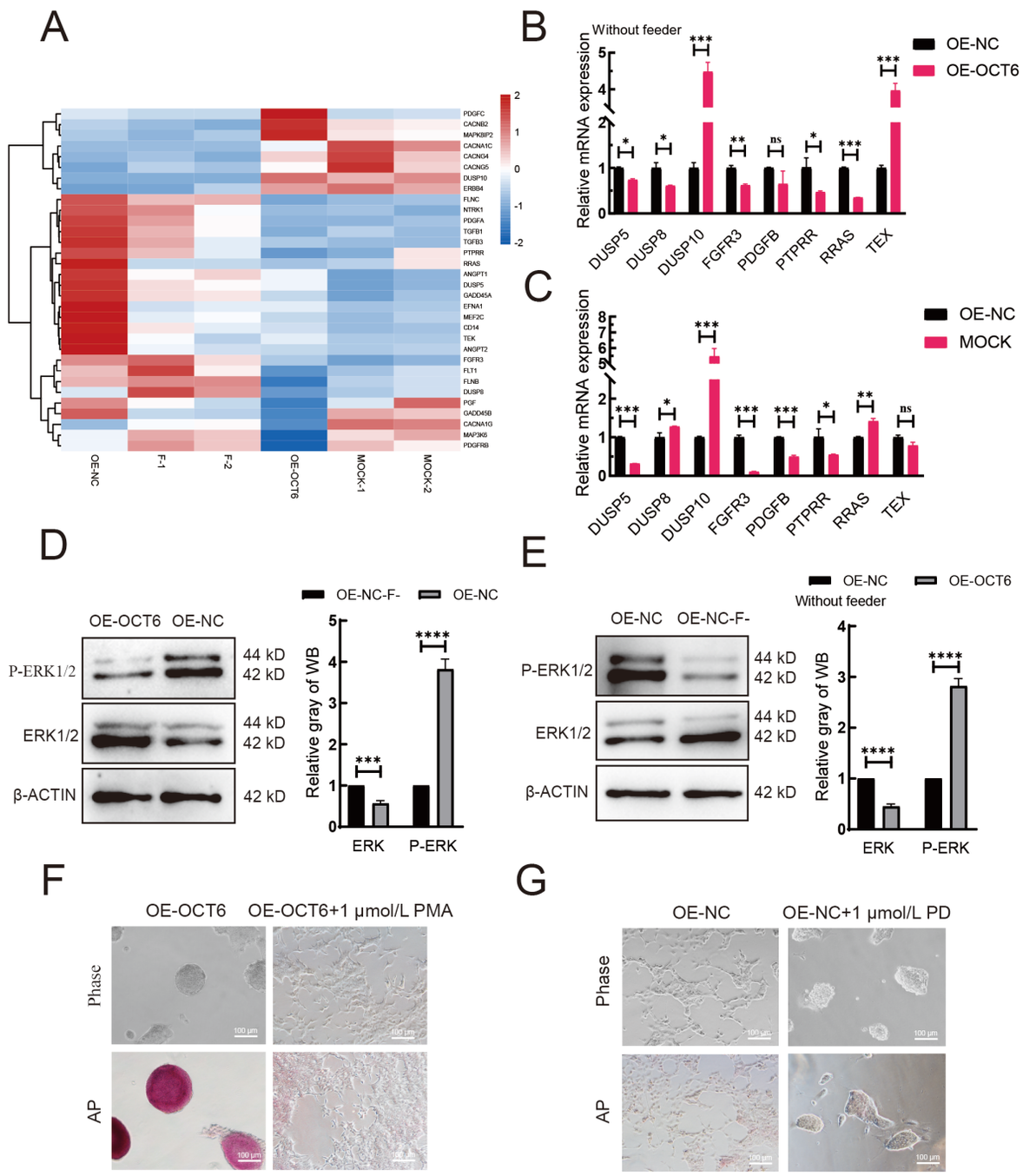

Figure 3 *OCT6* maintains piPSC colony morphology by inhibiting MAPK/ERK signaling pathway

A: Heat-map of expression of genes involved in MAPK/ERK signaling pathway based on RNA-seq. MOCK-1 and MOCK-2 represent gene expression of piPSCs on feeders, F-1 and F-2 represent gene expression of piPSCs without feeders. B: mRNA expression of genes involved in regulating MAPK-ERK signaling pathway by qRT-PCR in overexpressed control (OE-NC) and overexpressed *OCT6* (OE-OCT6) groups without feeders. C: mRNA expression of genes involved in regulating MAPK-ERK signaling pathway by qRT-PCR in overexpressed control (OE-NC) and MOCK groups. Relative expression levels were normalized to β-actin. Data represent mean±*SE*; *n*=3 independent experiments. D: Left: protein expression levels of ERK1/2 and p-ERK1/2 in OE-NC and OE-OCT6 groups without feeders, detected by western blotting. Right: quantitative analysis of ERK1/2 and P-ERK1/2 protein expression levels in OE-NC and OE-OCT6 groups without feeders. E: Left: protein expression levels of ERK1/2 and p-ERK1/2 in OE-NC without feeders (OE-NC-F) and OE-NC group, detected by western blotting. Right: quantitative analysis of ERK1/2 and P-ERK1/2 protein expression levels in OE-NC-F and OE-NC groups. F: Representative images of bright field and AP-staining in OE-OCT6 group cultured with 1 μmol/L PMA for 5 days. *n*=3 independent experiments. Scale bar: 100 μm. G: Representative images of bright field and AP staining in OE-NC group cultured with 1 μmol/L PD for 5 days. *n*=3 independent experiments. Scale bar: 100 μm.

PI3K inhibitor LY294002, consistent with the addition of PD0325901 in the OE-NC group, resulting in colony reduction (Figure 4F). These results suggest that elevated AKT signaling maintains the pluripotency of piPSCs under differentiation conditions. After adding the PI3K activator 740Y-P to the OE-NC group, pluripotency also recovered under differentiation conditions (Figure 4G). Therefore, the PI3K/AKT signaling pathway is beneficial for maintaining piPSC pluripotency under differentiation. After the concentration gradient test, 5 μmol/L LY294002 and 5 μmol/L 740Y-P were selected as the optimum concentrations for PI3K inhibition and activation, respectively (Supplementary Figure S1C, D).

DISCUSSION

PiPSCs can be effectively obtained by transferring *OCT4*, *SOX*, *KLF4*, and *c-Myc* into porcine fetal fibroblasts using lentiviral vectors (Ezashi et al., 2009). However, existing culture systems cannot be maintained long-term without feeders (Montserrat et al., 2012). In the absence of feeders, existing piPSCs show obvious differentiation, indicating the existence of several defects in piPSCs compared with humans and mice (Esteban et al., 2009). Here, we attempted to modify gene expression patterns to create a piPSC line that can maintain pluripotency and colony morphology without feeders. We found that introduction of the *OCT6* gene enabled piPSCs to achieve maintenance with no xenogeneic cells.

OCT6 and *OCT4* are both members of the POU family. To date, however, most studies have focused on their functions in neurons and neural progenitor cells (Kawasaki et al., 2003). Although the structures of OCT6 and OCT4 are similar, the reprogramming response is weaker in OCT6 (Jerabek et al., 2017). *OCT6* can cause extensive chromatin opening (Malik et al., 2019) and is reported to be expressed in early embryos (Meijer et al., 1990). As a pluripotency inducer, *OCT6* may play a potential role in the maintenance of pluripotency. Interestingly, in the present study, after *OCT6* overexpression, piPSCs maintained their pluripotency without feeders, and their expression pattern was essentially the same as regular piPSCs cultured on feeders. Differentiation-related gene expression (e.g., *L1CAM* (Bao et al., 2008)) and cell adhesion and ECM-related gene expression (e.g., *ITGB4* (Zhang et al., 2020b), *LPAR1* (Li et al., 2017a)) were decreased and enhanced, respectively, which was beneficial for the maintenance of piPSC colony morphology. The expression of *c-Myc* also increased, which may provide additional maintenance of self-renewal and pluripotency of piPSCs.

Our study showed that *OCT6* regulated the MAPK-ERK and PI3K-AKT pathways to help maintain piPSC pluripotency. Inhibition of MAPK signaling can induce PSCs to transform into the immature state (Hackett & Surani, 2014). There are many conflicting reports regarding the role of the MAPK signal transduction pathway in human embryonic stem cells (hESCs), including maintenance of pluripotency (Armstrong et al., 2006) and promotion of differentiation (Ding et al., 2010). In pigs, inhibition of MAPK can lead to the rapid loss of pluripotency (Gao et al., 2014). Furthermore, when *OCT6* is overexpressed, the expression of *DUSP10* (Hiratsuka et al., 2020) increases significantly, whereas the expression *PTPRR* (Su et al., 2013), *RRAS* (Michael et al., 2016), and *FGFR3* (Blick et al., 2013) decreases significantly, potentially inhibiting ERK. Surprisingly, under feeder withdrawal-stimulated differentiation, we found that low-dose PD0325901 led to colony formation, although proliferation ability was significantly decreased. Furthermore, the addition of a MAPK activator abolished the effects of *OCT6*, resulting in complete differentiation of piPSCs.

Activation of PI3K caused by *OCT6* overexpression can overcome the damage caused by inhibition of MAPK (Singh et al., 2012). As an important pathway for controlling ESC function, PI3K-AKT signaling plays a crucial role in cell self-renewal and pluripotency maintenance in pigs (Welham et al., 2011). Here, we found that overexpression of *OCT6* significantly activated the PI3K-AKT signaling pathway, with an increase in *MAGI1/2* (Zhang et al., 2020a), *LPAR1* (Cui et al., 2019), and *ITGB4* (Leng et al., 2016) gene expression, and decrease in *PPP2R3A* gene expression (Chen et al., 2019). These genes can promote PI3K-AKT signaling pathway activation. When PI3K-AKT signaling pathway inhibitors were added to the OE-OCT6 group, pluripotency was lost, and clones became smaller. These results indicate that inhibition of the PI3K-AKT signaling pathway damages piPSC pluripotency, suggesting that *OCT6* maintains piPSC pluripotency in the differentiated state via the PI3K-AKT signaling pathway.

Taken together, our results showed that overexpression of *OCT6* enhanced piPSC colony formation in the differentiated state and enhanced piPSC pluripotency, primarily by inhibition of the MAPK-ERK signaling pathway and activation of the PI3K-AKT signaling pathway.

It is worth highlighting that the genetically engineered (OE-OCT6) iPSCs, whose capability to differentiate *in vitro* was considerably attenuated by transgenically increasing the relative abundance of *OCT6* transcripts and extrinsic OCT6 proteins, may provide an excellent source of nuclear donor cells (NDCs) suitable for somatic cell nuclear transfer (SCNT)-based assisted reproductive technologies in pigs and other mammalian species (Gorczyca et al., 2021; Olivera et al., 2016; Samiec & Skrzyszowska, 2010; Secher et al., 2017; Zhang et al., 2014). Highly reprogrammable NDCs may exhibit an enhanced capacity to sustainably perpetuate stemness- and pluripotency-related molecular attributes. The latter, in turn, could enhance the epigenetic dedifferentiation capacity of OE-OCT6 iPSCs in SCNT-derived embryos, conceptuses, and progenies generated for transgenic and biomedical research, not only for pig-to-human xenotransplantation and tissue engineering, but also for regenerative and reconstructive surgical treatments in humans and other mammalian species (Berthelsen et al., 2021; Podstawski et al., 2022; Song et al., 2016; Wiater et al., 2021a, 2021b; Xu et al., 2022; Yu et al., 2021; Zhao et al., 2020).

DATA AVAILABILITY

Raw sequencing reads were deposited in the NCBI Sequence Read Archive (SRA) database (BioProjectID PRJNA854625), GSA database (PRJCA011011), and Science Data Bank database (DOI: 31253.11.sciencedb.j00139.00029).

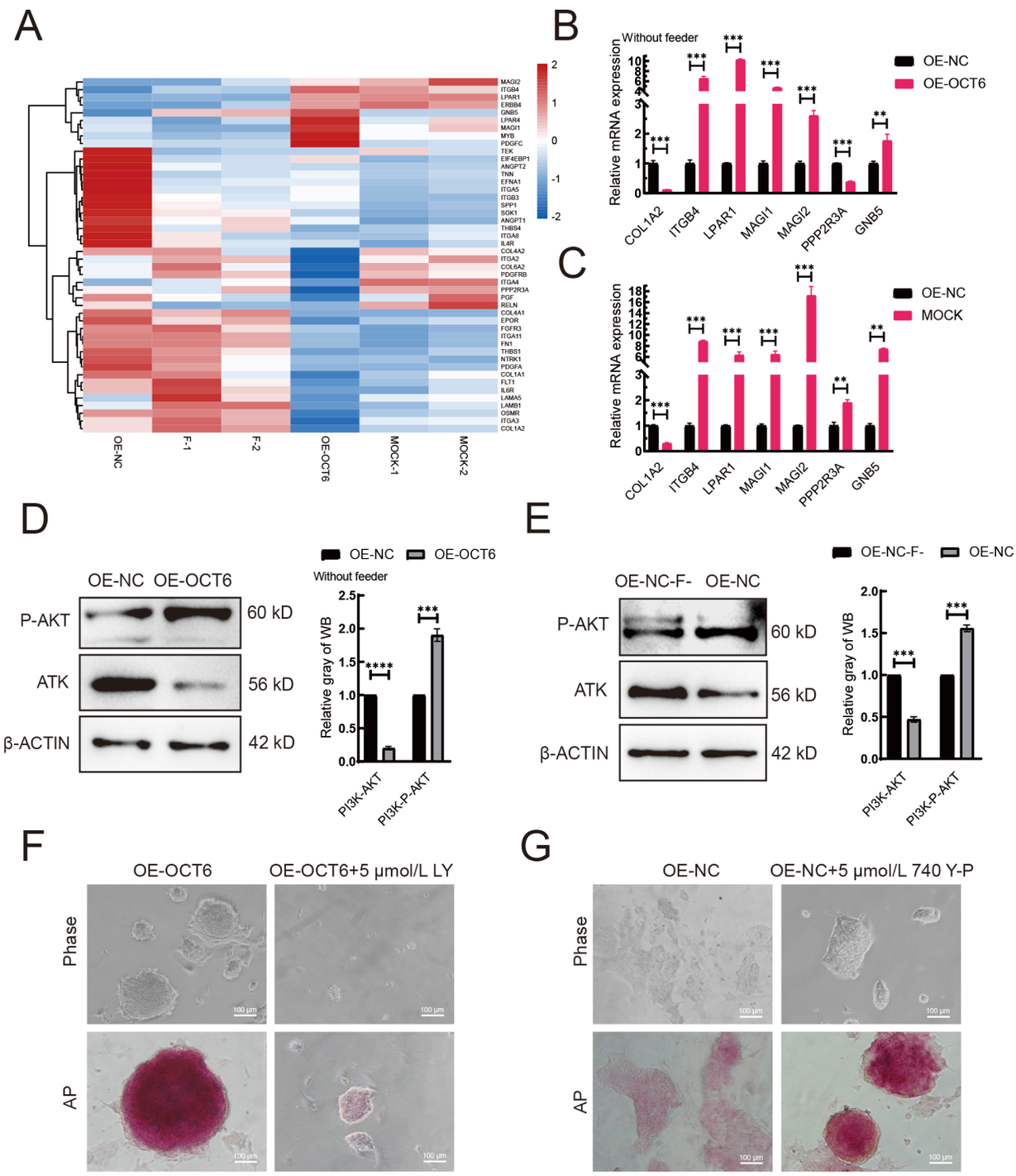

Figure 4 *OCT6* counteracts the negative effects of ERK inhibition on pluripotency by activating the PI3K-AKT signaling pathway

A: Heat-map of expression of genes involved in PI3K-AKT signaling pathway based on RNA-seq. B: mRNA of genes regulating PI3K-AKT signaling pathway detected by qRT-PCR in OE-NC and OE-OCT6 without feeders. C: mRNA of genes regulating PI3K-AKT signaling pathway detected by qRT-PCR in OE-NC and MOCK. Relative expression levels were normalized to β-actin. Data represent mean±SE; *n*=3 independent experiments. D: Left: protein expression levels of PI3K-AKT and p-PI3K-AKT in OE-NC and OE-OCT6 groups without feeders, detected by western blotting. Right: quantitative analysis of PI3K-AKT and p-PI3K-AKT protein expression levels in OE-NC and OE-OCT6 groups without feeders. E: Left: protein expression levels of PI3K-AKT and P-PI3K-AKT in OE-NC without feeders (OE-NC-F) and OE-NC group, detected by western blotting. Right: quantitative analysis of PI3K-AKT and p-PI3K-AKT protein expression levels in OE-NC-F and OE-NC groups. F: Representative images of bright field and AP-staining of OE-OCT6 piPSCs with 5 μmol/L LY for 5 days. *n*=3 independent experiments. Scale bar: 100 μm. G: Representative images of bright field and AP-staining of OE-OCT6 piPSCs with 5 μmol/L 740 Y-P for 5 days. *n*=3 independent experiments. Scale bar: 100 μm.

SUPPLEMENTARY DATA

Supplementary data to this article can be found online.

COMPETING INTERESTS

The authors declare that they have no competing interests.

AUTHORS' CONTRIBUTIONS

X.C.Y., X.L.W., and J.L.H. designed the research. X.C.Y., X.L.W., W.H.L., and X.J.W. performed the research. X.C.Y. and X.L.W. wrote the paper. X.C.Y., Q.Y.S., Y.X.L., and S.P. analyzed the data. X.C.Y. and X.L.W. modified the manuscript. All authors read and approved the final version of the manuscript.

ACKNOWLEDGMENTS

The authors thank Dr. Yong Tang for help revising the manuscript, and Dr. Zhen-Shuo Zhu and Ju-Qing Zhang for helpful comments on this paper.

REFERENCES

Aoki M, Fujishita T. 2017. Oncogenic roles of the PI3K/AKT/mTOR axis. *In*: Hunter E, Bister K. Viruses, Genes, and Cancer. Cham: Springer, 153–189.

Armstrong L, Hughes O, Yung S, Hyslop L, Stewart R, Wappler I, et al. 2006. The role of PI3K/AKT, MAPK/ERK and NFκβ signalling in the maintenance of human embryonic stem cell pluripotency and viability highlighted by transcriptional profiling and functional analysis. *Human Molecular Genetics*, **15**(11): 1894−1913.

Baghdadi MB, Castel D, Machado L, Fukada SI, Birk DE, Relaix F, et al. 2018. Reciprocal signalling by Notch-Collagen V-CALCR retains muscle stem cells in their niche. *Nature*, **557**(7707): 714−718.

Bao SD, Wu QL, Li ZZ, Sathornsumetee S, Wang H, McLendon RE, et al. 2008. Targeting cancer stem cells through L1CAM suppresses glioma growth. *Cancer Research*, **68**(15): 6043−6048.

Berthelsen MF, Riedel M, Cai HQ, Skaarup SH, Alstrup AKO, Dagnæs-Hansen F, et al. 2021. The CRISPR/Cas9 minipig-a transgenic minipig to produce specific mutations in designated tissues. *Cancers*, **13**(12): 3024.

Blick C, Ramachandran A, Wigfield S, McCormick R, Jubb A, Buffa FM, et al. 2013. Hypoxia regulates FGFR3 expression via HIF-1α and miR-100 and contributes to cell survival in non-muscle invasive bladder cancer. *British Journal of Cancer*, **109**(1): 50−59.

Chen J, Shu S, Chen YT, Liu Z, Yu LJ, Yang LX, et al. 2019. AIM2 deletion promotes neuroplasticity and spatial memory of mice. *Brain Research Bulletin*, **152**: 85−94.

Choi J, Huebner AJ, Clement K, Walsh RM, Savol A, Lin KX, et al. 2017. Prolonged Mek1/2 suppression impairs the developmental potential of embryonic stem cells. *Nature*, **548**(7666): 219−223.

Corsinotti A, Wong FCK, Tatar T, Szczerbinska I, Halbritter F, Colby D, et al. 2017. Distinct SoxB1 networks are required for naïve and primed pluripotency. *eLife*, **6**: e27746.

Cui R, Cao GM, Bai HM, Zhang ZY. 2019. LPAR1 regulates the development of intratumoral heterogeneity in ovarian serous cystadenocarcinoma by activating the PI3K/AKT signaling pathway. *Cancer Cell International*, **19**: 201.

Ding VMY, Ling L, Natarajan S, Yap MGS, Cool SM, Choo ABH. 2010. FGF-2 modulates Wnt signaling in undifferentiated hESC and iPS cells through activated PI3-K/GSK3β signaling. *Journal of Cellular Physiology*, **225**(2): 417−428.

Esteban MA, Xu JY, Yang JY, Peng MX, Qin DJ, Li W, et al. 2009. Generation of induced pluripotent stem cell lines from Tibetan miniature pig. *Journal of Biological Chemistry*, **284**(26): 17634−17640.

Ezashi T, Telugu BPVL, Alexenko AP, Sachdev S, Sinha S, Roberts RM. 2009. Derivation of induced pluripotent stem cells from pig somatic cells. *Proceedings of the National Academy of Sciences of the United States of America*, **106**(27): 10993−10998.

Friedrich RP, Schlierf B, Tamm ER, Bösl MR, Wegner M. 2005. The class III POU domain protein Brn-1 can fully replace the related Oct-6 during schwann cell development and myelination. *Molecular and Cellular Biology*, **25**(5): 1821−1829.

Gao Y, Guo YJ, Duan AQ, Cheng D, Zhang SQ, Wang HY. 2014. Optimization of culture conditions for maintaining porcine induced pluripotent stem cells. *DNA and Cell Biology*, **33**(1): 1−11.

Gong CC, Hu Y, Zhou M, Yao MJ, Ning ZX, Wang Z, et al. 2019. Identification of specific modules and hub genes associated with the progression of gastric cancer. *Carcinogenesis*, **40**(10): 1269−1277.

Gorczyca G, Wartalski K, Wiater J, Samiec M, Tabarowski Z, Duda M. 2021. Anabolic steroids-driven regulation of porcine ovarian putative stem cells favors the onset of their neoplastic transformation. *International Journal of Molecular Sciences*, **22**(21): 11800.

Hackett JA, Surani MA. 2014. Regulatory principles of pluripotency: from the ground state up. *Cell Stem Cell*, **15**(4): 416−430.

Haddadi N, Lin YG, Travis G, Simpson AM, Nassif NT, McGowan EM. 2018. PTEN/PTENP1: 'Regulating the regulator of RTK-dependent PI3K/Akt signalling', new targets for cancer therapy. *Molecular Cancer*, **17**(1): 37.

Hiratsuka T, Bordeu I, Pruessner G, Watt FM. 2020. Regulation of ERK basal and pulsatile activity control proliferation and exit from the stem cell compartment in mammalian epidermis. *Proceedings of the National Academy of Sciences of the United States of America*, **117**(30): 17796−17807.

Jauch R, Choo SH, Ng CKL, Kolatkar PR. 2011. Crystal structure of the dimeric oct6 (POU3f1) POU domain bound to palindromic more DNA. *Proteins*, **79**(2): 674−677.

Jerabek S, Ng CKL, Wu GM, Arauzo-Bravo MJ, Kim KP, Esch D, et al. 2017. Changing POU dimerization preferences converts oct6 into a pluripotency inducer. *EMBO Reports*, **18**(2): 319−333.

Kawasaki T, Oka N, Tachibana H, Akiguchi I, Shibasaki H. 2003. oct6, a transcription factor controlling myelination, is a marker for active nerve regeneration in peripheral neuropathies. *Acta Neuropathologica*, **105**(3): 203−208.

Kim KP, Choi J, Yoon J, Bruder JM, Shin B, Kim J, et al. 2021. Permissive epigenomes endow reprogramming competence to transcriptional regulators. *Nature Chemical Biology*, **17**(1): 47−56.

Kim KP, Wu Y, Yoon J, Adachi K, Wu GM, Velychko S, et al. 2020. Reprogramming competence of OCT factors is determined by transactivation domains. *Science Advances*, **6**(36): eaaz7364.

Kuhlbrodt K, Herbarth B, Sock E, Enderich J, Hermans-Borgmeyer I, Wegner M. 1998. Cooperative function of POU proteins and SOX proteins in glial cells. *Journal of Biological Chemistry*, **273**(26): 16050−16057.

Leng C, Zhang ZG, Chen WX, Luo HP, Song J, Dong W, et al. 2016. An integrin beta4-EGFR unit promotes hepatocellular carcinoma lung metastases by enhancing anchorage independence through activation of

FAK-AKT pathway. *Cancer Letters*, **376**(1): 188−196.

Li N, Yan YL, Fu S, Li RJ, Zhao PF, Xu XY, et al. 2017a. Lysophosphatidic acid enhances human umbilical cord mesenchymal stem cell viability without differentiation via LPA receptor mediating manner. *Apoptosis*, **22**(10): 1296−1309.

Li XL, Liu L, Li DD, He YP, Guo LH, Sun LP, et al. 2017b. Integrin β4 promotes cell invasion and epithelial-mesenchymal transition through the modulation of Slug expression in hepatocellular carcinoma. *Scientific Reports*, **7**: 40464.

Li ZY, Li XH, Tian GW, Zhang DY, Gao H, Wang ZY. 2019. MAGI1 inhibits the proliferation, migration and invasion of glioma cells. *OncoTargets and Therapy*, **12**: 11281−11290.

Ma YY, Yu T, Cai YX, Wang HY. 2018. Preserving self-renewal of porcine pluripotent stem cells in serum-free 3i culture condition and independent of LIF and b-FGF cytokines. *Cell Death Discovery*, **4**: 21.

Malik V, Glaser LV, Zimmer D, Velychko S, Weng MX, Holzner M, et al. 2019. Pluripotency reprogramming by competent and incompetent POU factors uncovers temporal dependency for Oct4 and Sox2. *Nature Communications*, **10**(1): 3477.

Mansouri A, Hallonet M, Gruss P. 1996. *Pax* genes and their roles in cell differentiation and development. *Current Opinion in Cell Biology*, **8**(6): 851−857.

Meijer D, Graus A, Kraay R, Langeveld A, Mulder MP, Grosveld G. 1990. The octamer binding factor oct6: cDNA cloning and expression in early embryonic cells. *Nucleic Acids Research*, **18**(24): 7357−7365.

Michael JV, Wurtzel JGT, Goldfinger LE. 2016. Regulation of H-Ras-driven MAPK signaling, transformation and tumorigenesis, but not PI3K signaling and tumor progression, by plasma membrane microdomains. *Oncogenesis*, **5**(5): e228.

Montserrat N, De Oñate L, Garreta E, Gonzãlez F, Adamo A, Eguizãbal C, et al. 2012. Generation of feeder-free pig induced pluripotent stem cells without Pou5f1. *Cell Transplantation*, **21**(5): 815−825.

Oh GS, Yoon J, Kim G, Kim GH, Kim DS, Choi B, et al. 2020. Regulation of adipocyte differentiation by clusterin-mediated Krüppel-like factor 5 stabilization. *The FASEB Journal*, **34**(12): 16276−16290.

Olivera R, Moro LN, Jordan R, Luzzani C, Miriuka S, Radrizzani M, et al. 2016. *In vitro* and *in vivo* development of horse cloned embryos generated with iPSCs, mesenchymal stromal cells and fetal or adult fibroblasts as nuclear donors. *PLoS One*, **11**(10): e0164049.

Podstawski P, Samiec M, Skrzyszowska M, Szmatoła T, Semik-Gurgul E, Ropka-Molik K. 2022. The induced expression of *BPV E4* gene in equine adult dermal fibroblast cells as a potential model of skin sarcoid-like Neoplasia. *International Journal of Molecular Sciences*, **23**(4): 1970.

Samiec M, Skrzyszowska M. 2010. Preimplantation developmental capability of cloned pig embryos derived from different types of nuclear donor somatic cells. *Annals of Animal Science*, **10**(4): 385−398.

Secher JO, Liu Y, Petkov S, Luo YL, Li D, Hall VJ, et al. 2017. Evaluation of porcine stem cell competence for somatic cell nuclear transfer and production of cloned animals. *Animal Reproduction Science*, **178**: 40−49.

Singh AM, Reynolds D, Cliff T, Ohtsuka S, Mattheyses AL, Sun YH, et al. 2012. Signaling network crosstalk in human pluripotent cells: a Smad2/3-regulated switch that controls the balance between self-renewal and differentiation. *Cell Stem Cell*, **10**(3): 312−326.

Sock E, Enderich J, Rosenfeld MG, Wegner M. 1996. Identification of the nuclear localization signal of the POU domain protein Tst-1/oct6. *Journal of Biological Chemistry*, **271**(29): 17512−17518.

Son YS, Seong RH, Ryu CJ, Cho YS, Bae KH, Chung SJ, et al. 2011. Brief report: L1 cell adhesion molecule, a novel surface molecule of human embryonic stem cells, is essential for self-renewal and pluripotency. *Stem Cells*, **29**(12): 2094−2099.

Song H, Li H, Huang MR, Xu D, Wang ZY, Wang F. 2016. Big animal cloning using transgenic induced pluripotent stem cells: a case study of goat transgenic induced pluripotent stem cells. *Cellular Reprogramming*, **18**(1): 37−47.

Su PH, Lin YW, Huang RL, Liao YP, Lee HY, Wang HC, et al. 2013. Epigenetic silencing of PTPRR activates MAPK signaling, promotes metastasis and serves as a biomarker of invasive cervical cancer. *Oncogene*, **32**(1): 15−26.

Teichroeb JH, Betts DH, Vaziri H. 2011. Suppression of the imprinted gene *NNAT* and X-chromosome gene activation in isogenic human iPS cells. *PLoS One*, **6**(10): e23436.

Wei YD, Du XM, Yang DH, Ma FL, Yu XW, Zhang MF, et al. 2021. Dmrt1 regulates the immune response by repressing the TLR4 signaling pathway in goat male germline stem cells. *Zoological Research*, **42**(1): 14−27.

Welham MJ, Kingham E, Sanchez-Ripoll Y, Kumpfmueller B, Storm M, Bone H. 2011. Controlling embryonic stem cell proliferation and pluripotency: the role of PI3K- and GSK-3-dependent signalling. *Biochemical Society Transactions*, **39**(2): 674−678.

Wen XM, Jiao LD, Tan H. 2022. MAPK/ERK pathway as a central regulator in vertebrate organ regeneration. *International Journal of Molecular Sciences*, **23**(3): 1464.

Wiater J, Samiec M, Skrzyszowska M, Lipiński D. 2021a. Trichostatin A-assisted epigenomic modulation affects the expression profiles of not only recombinant human α1, 2-fucosyltransferase and α-galactosidase A enzymes but also Galα1→3Gal epitopes in porcine Bi-transgenic adult cutaneous fibroblast cells. *International Journal of Molecular Sciences*, **22**(3): 1386.

Wiater J, Samiec M, Wartalski K, Smorąg Z, Jura J, Słomski R, et al. 2021b. Characterization of mono- and Bi-transgenic pig-derived epidermal keratinocytes expressing human *FUT2* and *GLA* genes-in vitro studies. *International Journal of Molecular Sciences*, **22**(18): 9683.

Wolfrum K, Wang Y, Prigione A, Sperling K, Lehrach H, Adjaye J. 2010. The LARGE principle of cellular reprogramming: lost, acquired and retained gene expression in foreskin and amniotic fluid-derived human iPS cells. *PLoS One*, **5**(10): e13703.

Wu DY, Yao Z. 2005. Isolation and characterization of the murine *Nanog* gene promoter. *Cell Research*, **15**(5): 317−324.

Wu X, Oatley JM, Oatley MJ, Kaucher AV, Avarbock MR, Brinster RL. 2010. The POU domain transcription factor POU3F1 is an important intrinsic regulator of GDNF-induced survival and self-renewal of mouse spermatogonial stem cells. *Biology of Reproduction*, **82**(6): 1103−1111.

Wu XL, Zhu ZS, Xiao X, Zhou Z, Yu S, Shen QY, et al. 2021. *LIN28A* inhibits *DUSP* family phosphatases and activates MAPK signaling pathway to maintain pluripotency in porcine induced pluripotent stem cells. *Zoological Research*, **42**(3): 377−388.

Xu JJ, Yu LQ, Guo JX, Xiang JZ, Zheng Z, Gao DF, et al. 2019. Generation of pig induced pluripotent stem cells using an extended pluripotent stem cell culture system. *Stem Cell Research & Therapy*, **10**(1): 193.

Xu K, Zhang XL, Liu ZG, Ruan JX, Xu CJ, Che JJ, et al. 2022. A transgene-free method for rapid and efficient generation of precisely edited pigs without monoclonal selection. *Science China Life Sciences*, **65**(8): 1535−1546.

Yao X, Tan Z, Gu B, Wu RR, Liu YK, Dai LC, et al. 2010. Promotion of self-renewal of embryonic stem cells by midkine. *Acta Pharmacologica Sinica*, **31**(5): 629−637.

Yu JH, Liu D, Sun XJ, Yang K, Yao JF, Cheng C, et al. 2019. CDX2 inhibits the proliferation and tumor formation of colon cancer cells by suppressing Wnt/β-catenin signaling via transactivation of GSK-3β and Axin2 expression. *Cell Death & Disease*, **10**(1): 26.

Yu XW, Li TT, Du XM, Shen QY, Zhang MF, Wei YD, et al. 2021. Single-cell RNA sequencing reveals atlas of dairy goat testis cells. *Zoological Research*, **42**(4): 401−405.

Zhang G, Chen HX, Yang SN, Zhao J. 2020a. MAGI1-IT1 stimulates proliferation in non-small cell lung cancer by upregulating AKT1 as a ceRNA. *European Review for Medical and Pharmacological Sciences*, **24**(2): 691−698.

Zhang R, Yu S, Shen QY, Zhao WX, Zhang JQ, Wu XL, et al. 2021. AXIN2 reduces the survival of porcine induced pluripotent stem cells (piPSCs). *International Journal of Molecular Sciences*, **22**(23): 12954.

Zhang WJ, Zhang XY, Zhang L, Xu D, Cheng NN, Tang Y, et al. 2020b. Astrocytes increase exosomal secretion of oligodendrocyte precursor cells to promote their proliferation via integrin β4-mediated cell adhesion. *Biochemical and Biophysical Research Communications*, **526**(2): 341−348.

Zhang Y, Wei C, Zhang PF, Li X, Liu T, Pu Y, et al. 2014. Efficient reprogramming of naïve-like induced pluripotent stem cells from porcine adipose-derived stem cells with a feeder-independent and serum-free system. *PLoS One*, **9**(1): e85089.

Zhao H, Li YY, Wiriyahdamrong T, Yuan ZM, Qing YB, Li HH, et al. 2020. Improved production of GTKO/hCD55/hCD59 triple-gene-modified *Diannan* miniature pigs for xenotransplantation by recloning. *Transgenic Research*, **29**(3): 369−379.

Zhu ZS, Wu XL, Li Q, Zhang JQ, Yu S, Shen QY, et al. 2021. Histone demethylase complexes KDM3A and KDM3B cooperate with OCT4/SOX2 to define a pluripotency gene regulatory network. *The FASEB Journal*, **35**(6): e21664.